Molecular evidence that the Channel Islands populations of the orange-crowned warbler (*Oreothlypis celata*; Aves: Passeriformes: Parulidae) represent a distinct evolutionary lineage

We used molecular data to assess the degree of genetic divergence across the breeding range of the orange-crowned warbler (*Oreothlypis celata*) in western North America with particular focus on characterizing the divergence between *O. celata* populations on the mainland of southern California and on the Channel Islands. We obtained sequences of the mitochondrial gene *ND2* and genotypes at ten microsatellite data for 192 *O. celata* from populations spanning all four recognized subspecies. We recovered low levels of divergence between *O. celata* populations and genetic patterns were consistent with isolation by distance. However, populations on the Channel Islands were genetically divergent from those on the mainland. We found evidence for greater gene flow from the Channel Islands population to mainland southern California than from the mainland to the islands. We discuss these data in the context of differentiation in phenotypic and ecological characters.

PeerJ Preprints | https://doi.org/10.7287/peerj.preprints.27418v1 | CC BY 4.0 Open Access | rec: 7 Dec 2018, publ: 7 Dec 2018

Molecular evidence that the Channel Islands populations of the orange-crowned warbler (*Oreothlypis celata*; Aves: Passeriformes: Parulidae) represent a distinct evolutionary lineage

Zachary R Hanna [1, 2], **Carla Cicero** [Corresp., 1], **Rauri CK Bowie** [Corresp. 1, 2]

[1] Museum of Vertebrate Zoology, University of California, Berkeley, Berkeley, California, United States of America

[2] Department of Integrative Biology, University of California, Berkeley, Berkeley, California, United States of America

Corresponding Authors: Carla Cicero, Rauri CK Bowie
Email address: ccicero@berkeley.edu, bowie@berkeley.edu

We used molecular data to assess the degree of genetic divergence across the breeding range of the orange-crowned warbler (*Oreothlypis celata*) in western North America with particular focus on characterizing the divergence between *O. celata* populations on the mainland of southern California and on the Channel Islands. We obtained sequences of the mitochondrial gene *ND2* and genotypes at ten microsatellite data for 192 *O. celata* from populations spanning all four recognized subspecies. We recovered low levels of divergence between *O. celata* populations and genetic patterns were consistent with isolation by distance. However, populations on the Channel Islands were genetically divergent from those on the mainland. We found evidence for greater gene flow from the Channel Islands population to mainland southern California than from the mainland to the islands. We discuss these data in the context of differentiation in phenotypic and ecological characters.

Introduction

Oceanic islands have served as a natural laboratory for evolutionary studies for decades (Crawford, 2012). Patterns of phenotypic and genetic divergence on islands with varying degrees of isolation shed light on the processes of adaptation and speciation (Losos & Ricklefs, 2009; Greenberg & Danner, 2013) and provide data for evaluating traits that promote biodiversity (Lomolino, 2005; Gunderson, Mahler & Leal, 2018). Furthermore, comparisons of island taxa and their mainland counterparts are fundamental to assessing the taxonomic status of island endemics, many of which are of conservation concern (Wilson et al., 2009).

The California Channel Islands are well-known for their endemic or near endemic species and subspecies of birds (Johnson, 1972; Jones & Diamond, 1976). Of the forty-one native land bird species found on these islands, thirteen (32%) show phenotypic differentiation between the islands and mainland (Johnson, 1972). The islands are divided into two groups that differ geologically and biologically: the northern islands (San Miguel, Santa Rosa, Santa Cruz, and Anacapa) and the southern islands (San Nicolas, Santa Barbara, Santa Catalina, and San Clemente). Together, they extend for 260 km off the coast of southern California and range between 20 and 98 km from the mainland (Schoenherr, Feldmeth & Emerson, 1999). Patterns and processes of avian (especially passerine) diversification on the Channel Islands have been a topic of interest among ornithologists for decades (Diamond, 1969; Johnson, 1972; Lynch & Johnson, 1974; Greenberg & Danner, 2013). Apart from the following, few Channel Islands bird taxa have been the subject of published genetic studies: *Aphelocoma californica* and *A. insularis* (Delaney, Zafar & Wayne, 2008); *Melospiza melodia* (Wilson et al., 2009); *Lanius ludovicianus*, (Mundy, Winchell & Woodruff, 1997; Caballero & Ashley, 2011); *Eremophila alpestris* (Mason et al., 2014); and *Artemisiospiza belli* (Karin et al., 2018). Overall, these studies have shown that the Channel Islands harbor genetic distinctiveness in

avian populations and that levels of divergence and gene flow between the islands and mainland vary among taxa.

The orange-crowned warbler (*Oreothlypis celata*) is currently divided into four subspecies that differ in plumage color (Figures S1 and S2), size, molt patterns, habitat, and timing of migration and breeding (Foster, 1967; Gilbert, Sogge & Van Riper III, 2010). *Oreothlypis celata celata* (Say, 1823) breeds primarily in low, deciduous shrub-dominated thickets in northern North America, including most of Alaska through eastern Canada. *Oreothlypis celata lutescens* (Ridgway, 1872) prefers to nest in dense riparian chaparral with vertical structure provided by oaks or conifers along the Pacific coast from southeastern Alaska through California (Dunn & Garrett, 1997). *Oreothlypis celata sordida* (Townsend, 1890) nests in scrub and woodland on all eight California Channel Islands as well as on the Islas Coronado and Islas de Todos Santos off the northwestern coast of Baja California and in restricted areas on the coast of mainland southern California (Dunn & Garrett, 1997; Schoenherr, Feldmeth & Emerson, 1999). *Oreothlypis celata orestera* (Oberholser, 1905) nests in dense riparian areas and, at higher elevations, in stands of aspen groves in the Rocky Mountains from northern British Columbia through southern New Mexico and in the western deserts of North America and (Dunn & Garrett, 1997).

Analyzing the geographic differentiation and distribution patterns of Channel Island birds, Johnson (1972) found evidence of both single and multiple colonization events, depending on the particular taxon. For *Oreothlypis celata*, he hypothesized that the insular *O. c. sordida* originated from a single colonization from the mainland to the northern Channel Islands, followed by differentiation and subsequent dispersal among the islands and recolonization of the mainland in areas that were locally unsuitable for *O. c. lutescens*. He also hypothesized that *O. c.*

sordida is more closely related to Rocky Mountain *O. c. orestera* populations than to Pacific coast *O. c. lutescens* populations, suggesting a relictual pattern of evolution and distribution.

In the only published genetic study of *Oreothlypis celata*, Bull et al. (2010) used mitochondrial DNA (mtDNA) and microsatellite data to assess the relationships between northwestern North American populations of *Oreothlypis celata celata* and *O. c. lutescens* on Haida Gwaii, Canada. They found low, but statistically significant, differentiation between populations, suggesting recent divergence. They also found a pattern consistent with isolation by distance. However, because Bull et al. (2010) did not include the other two *O. celata* subspecies (*O. c. orestera* and *O. c. sordida*) in their analyses, their data did not provide insight into broader patterns and processes of differentiation across the species, including between Channel Islands and mainland populations.

In order to analyze broad-scale divergences among populations, we sampled mitochondrial and nuclear genetic data from all four subspecies of *Oreothlypis celata*. We assessed the relationship between Channel Island and mainland southern California populations and determined the relative rates of migration between these populations to test Johnson's (1972) hypotheses about the origin and differentiation of *O. celata* on the Channel Islands. We discuss these data in the context of what is known about avian differentiation on the islands.

Materials and methods

Population sampling

We obtained blood and/or frozen tissue samples from 192 *Oreothlypis celata* individuals from western North America representing each of the four subspecies (Table S1 and Figure 1). We only used samples collected during the breeding months of early April through July (Gilbert, Sogge & Van Riper III, 2010) from 1983 to 2009 (Table S1). We also obtained frozen tissue

samples from two Nashville warblers (*Oreothlypis ruficapilla*) to use as outgroups in our analyses. We obtained samples from museum tissue collections (Table S1) and collected samples under California Department of Fish and Game scientific collecting permit numbers SC-458 and SC-10109, U.S. Fish and Wildlife Service permit number MB153526, and with permission from the UC Berkeley Animal Care and Use Committee under Animal Use Protocols R285 and R317.

We examined populations at several hierarchical levels. First, we analyzed the data using all of the samples without *a priori* groupings. When these initial analyses did not reveal spatial structure in the genetic data, we grouped the samples into eight populations (Figure 1) based on their geographic proximity. We then grouped the samples on either side of two separate geographic divisions: northern versus southern (populations 1-3 and 4-8, respectively, in Figure 1) and coastal versus interior (populations 2, 6-8 and 1, 3-5, respectively, in Figure 1). Our division between the northern and southern samples near the Pacific Coast fell at the southern limit of the Cascade Range in northern California. In the interior, we divided northern from southern samples between the Canadian Rocky Mountains and the Southern Rocky Mountains at the northern Idaho Clearwater River drainage. These landmarks are ecologically significant as they mark the southern extents of cedar-hemlock forest ecosystems (Brunsfeld et al., 2001) and have been hypothesized by many as sites of lineage contact in various taxa (Soltis et al., 1997; Swenson & Howard, 2005; Burg et al., 2006). We divided coastal from interior samples by designating as interior all areas east of the Alaska Range, Coast Mountains, the Cascades, and the Sierra Nevada as splits between coastal and interior populations have been hypothesized in other warbler taxa (Bermingham et al., 1992). Finally, we grouped samples based on the four existing subspecific designations. We utilized each of these four separate sample groupings in subsequent analyses.

Laboratory procedures

We extracted DNA from blood or frozen tissues using a DNeasy Blood & Tissue Kit (Qiagen, Hilden, Germany) following the Qiagen protocol for animal tissues. We sequenced the mitochondrial genes NADH subunit 2 (*ND2*) and ATP Synthase subunit 6 (*ATP6*), both of which are commonly used in avian phylogeographic studies. We amplified a 1041 basepair (bp) fragment of the *ND2* gene using the polymerase chain reaction (PCR) with primers L5204 and H6312 (Sorenson et al., 1999). PCR reactions (10μL) contained 1X PCR Buffer (10mM Tris-HCl, 1.5 mM $MgCl_2$, 50 mM KCl, pH 8.3), 0.6 μM of each primer, 200 μM of each dNTP, 0.6 U of *Taq* and approximately 5-10 ng of genomic DNA. The PCR profile included an initial denaturation at 94ºC for 2 min; followed by 35 cycles of denaturation at 94ºC for 30 s, annealing at 53ºC for 30 s, and extension at 72ºC for 1 min; with a final extension at 72ºC for 10 min. We amplified a 704 bp fragment of the *ATP6* gene by PCR using the primers a8PWL and C03HMH (http://nmg.si.edu/bermlab.htm). The PCR profile followed that for the *ND2* gene, except for annealing at 54ºC and extension for 45 s during the 35 cycle phase before the final extension.

We purified the PCR products using Exonuclease I and Shrimp Alkaline Phosphatase (ExoSAP-IT™, Applied Biosystems, Waltham, Massachusetts, U.S.A.) and sequenced the purified products using Big Dye terminator chemistry v. 3.1 (Applied Biosystems) and an ABI PRISM 3730 DNA Analyzer (Applied Biosystems). We analyzed only samples for which we obtained sequences of both DNA strands. We aligned complementary DNA strands, edited all sequences, detected stop codons, and aligned consensus sequences using Sequencher version 4.7 (Gene Codes Corporation, Ann Arbor, Michigan, U.S.A.). After obtaining 704 bp of *ATP6* for 106 individuals, we detected the presence of a pseudogene in sequences and thus eliminated the *ATP6* gene from further analyses.

We used ten polymorphic microsatellite markers (Vce34, Vce50, Vce70, Vce102, Vce103, Vce109, Vce116, Vce128, Vce167, and Vce179) developed for *O. celata* (Bowie et al., 2017). All ten loci were tetranucleotide repeats and three of them had imperfect core repeats. We amplified these microsatellites using PCR in 10 µL reactions containing: 1x PCR Buffer (10mM Tris-HCl, 1.5 mM $MgCl_2$, 50 mM KCl, pH 8.3), 0.6 µM of each primer, 200 µM of each dNTP, 0.6 U of *Taq* and approximately 5-10 ng of genomic DNA. The PCR conditions included one denaturation cycle at 94ºC for 2 min and 30 cycles consisting of 15 s of denaturation at 94ºC, 15 s of annealing at 50-55ºC, and 15 s of extension at 72ºC. We used T4 DNA polymerase (New England Biolabs, Ipswich, Massachusetts, U.S.A.) treatment to clean the PCR products of the Vce34, Vce50, Vce102, Vce103, Vce128, and Vce179 markers (Ginot et al., 1996). We mixed the samples with formamide and GS-500 LIZ size standard (Applied Biosystems) and analyzed them using an ABI PRISM 3730 DNA Analyzer. We conducted allele binning and genotyping using Genemapper version 4.0 (Applied Biosystems).

Mitochondrial DNA analyses

We analyzed the *ND2* sequences using maximum likelihood (ML), neighbor-joining (NJ), and maximum parsimony (MP) algorithms. We used RAxML BlackBox (Stamatakis, Hoover & Rougemont, 2008) to construct an ML tree with 100 bootstrap replicates and PAUP* version 4.0b10 (Swofford, 2003) to construct NJ and MP trees. Preliminary analyses of the mtDNA data using NJ, ML, and MP algorithms were not informative and intraspecific datasets often do not comply with the assumptions of MP and ML algorithms (Posada & Crandall, 2001). Therefore, we did not further explore tree-building methods that assume bifurcation of lineages by default and instead focused on the population genetics approaches described hereafter.

We generated a statistical parsimony network using TCS version 1.01 (Clement, Posada & Crandall, 2000) to visualize relationships among haplotypes and to analyze phylogeographic structure. In addition, we used analysis of molecular variance (AMOVA) in Arlequin version 3.1 (Excoffier, Smouse & Quattro, 1992; Excoffier, Laval & Schneider, 2007) to calculate the proportion of total mtDNA genetic variation explained by population groupings. The AMOVA provided estimates of overall F_{ST} and its analogue, Φ_{ST} (calculated using the Tamura-Nei model with a 0.05 gamma correction), using a non-parametric permutation approach to determine significance levels (Excoffier, Smouse & Quattro, 1992). We used Arlequin version 3.1 to examine genetic structure among population subdivisions by calculating pairwise F_{ST} and Φ_{ST} statistics (10,000 permutations) and applying sequential Bonferroni corrections when evaluating significance (Rice, 1989). We also used Arlequin version 3.1 to estimate haplotype diversity (*h)* and nucleotide diversity (π) (Nei, 1987), to calculate pairwise mismatch distributions for populations (Sum of Squared deviations and Harpending's Raggedness index calculated to test goodness of fit; 10,000 bootstrap replicates), and to run two tests of selective neutrality, Tajima's D (Tajima, 1989) and Fu's *F* (Fu, 1997) tests.

We performed a spatial analysis of molecular variance (SAMOVA) using SAMOVA 1.0 (Dupanloup, Schneider & Excoffier, 2002) to assess the geographic arrangement of genetic structure. Unlike an AMOVA, this method does not require an a priori definition of populations. Instead, it uses sequence and geographic coordinate data (Lambert projection) to maximize the proportion of total genetic variation between populations (Dupanloup, Schneider & Excoffier, 2002). We identified the most likely partitioning of the samples by running SAMOVA 1.0 repeatedly with 2 to 20 groups and looking for the division assemblage with a maximized F_{CT} (Dupanloup, Schneider & Excoffier, 2002).

Microsatellite analyses

We used Arlequin version 3.1 (Excoffier, Laval & Schneider, 2007) to calculate observed (H_O) and expected (H_E) heterozygosity values. We tested for Hardy-Weinberg equilibrium (HWE) and heterozygote deficiency using Genepop version 4.0.10 (10,000 dememorization steps, 1,000 batches, 10,000 iterations) (Raymond & Rousset, 1995; Rousset, 2008). In addition, we tested the microsatellite genotypes in each population and at each locus for linkage equilibrium using Genepop version 4.0.10 (10,000 dememorization steps, 1,000 batches, 10,000 iterations) (Raymond & Rousset, 1995), applying sequential Bonferroni corrections when evaluating significance (Rice, 1989). We examined null allele presence using Micro-Checker version 2.2.3 (Van Oosterhout et al., 2004) and used FSTAT version 2.9.3.2 (Goudet, 1995, 2001) to estimate allelic richness (R_s), which controls for sample size when comparing the number of alleles between populations (Leberg, 2002).

We tested the proportion of total genetic variance explained by population groupings by performing an AMOVA (Excoffier, Smouse & Quattro, 1992) in Arlequin version 3.1, which provided estimates of overall F_{ST}. We calculated the significance levels for the AMOVA using a non-parametric permutation approach (10,000 permutations) (Excoffier, Smouse & Quattro, 1992). We examined genetic structure among population subdivisions by calculating pairwise F_{ST} values using Arlequin version 3.1 (10,000 permutations) and pairwise R_{ST} values using RSTCALC version 2.2 (Goodman, 1997), applying sequential Bonferroni corrections for multiple simultaneous comparisons when evaluating significance (Rice, 1989).

We tested the pairwise correlation between direct geographic and genetic (Nei, 1972) distances (isolation by distance) among all individuals sampled by conducting a Mantel test using GenAlEx version 6.1 (Peakall & Smouse, 2006, 2012). We also used GenAlEx version 6.1

to run a principal coordinates analysis (PCA) in order to examine the organization of the genetic structure.

In a further effort to detect spatial organization in our sample assemblage, we analyzed our dataset of ten microsatellite loci using Structure version 2.3.4 (Pritchard, Stephens & Donnelly, 2000; Falush, Stephens & Pritchard, 2003; Hubisz et al., 2009; Pritchard, Falush & Hubisz, 2012). This method uses Bayesian clustering to examine genetic frequencies across loci and attempts to identify the number of clusters (*K*) based on the likelihood values for varying *K* values. We performed preliminary analyses without providing any information concerning population designations. After these initial analyses, we then designated eight populations in the input and used this information as a prior (LOCPRIOR) (Hubisz et al., 2009) in further analyses to improve population discrimination. We implemented the analyses using the admixture model with correlated allele frequencies (Falush, Stephens & Pritchard, 2003), examined *K*=1-20, executed a 100,000 MCMC iteration burn-in, and then performed 1,000,000 subsequent MCMC iterations. We replicated the simulation at each *K* twenty times. To assist in identifying the optimal *K*, we used Structure Harvester version 0.6.94 (Earl & vonHoldt, 2012; Earl, 2014), which uses the Evanno et al. (2005) method to identify the number of clusters. We ran Structure and Structure Harvester using StrAuto version 1.0 (Chhatre & Emerson, 2017, 2018) with GNU Parallel version 20141022 (Tange, 2011). To align clusters across the Structure runs, we ran CLUMPP version 1.1.2 (Jakobsson & Rosenberg, 2007) and then used a modified version of Distruct version 2.2 (Raj, Stephens & Pritchard, 2014; Chhatre, 2016; Hanna, Cicero & Bowie, 2018) to plot the clusters.

Based on the results of the Structure analysis described above, we ran two additional Structure analyses to check for the presence of substructure. We first analyzed the Channel

Islands samples with the samples from Santa Cruz Island and Santa Catalina Island split into separate populations. We used the parameters as detailed above, including the LOCPRIOR for *K*=1-10. We then analyzed the seven remaining populations with the same parameters as above for *K*=1-20.

In order to assess the relative rate of migration between the Channel Islands and mainland southern California, we ran IMa2p version 58a0260 (Sethuraman & Hey, 2015; Sethuraman, 2017). We input both the *ND2* sequences and microsatellite genotypes and performed three separate runs each with 15 chains, 1,000,000 burnin steps, and 2,000,000 further steps following the burnin. We have provided further methodology details in ocwa-popgen version 1.0.0 on GitHub (Hanna, Cicero & Bowie, 2018).

Results

mtDNA sequence variation

We obtained a complete 1041 bp fragment of the mtDNA *ND2* gene for 192 *Oreothlypis celata* and two *O. ruficapilla* individuals; there were no missing data and no insertions, deletions, or gaps. After merging identical sequences, we found 72 unique haplotypes (Appendix 1) with 81 variable sites. We found no evidence for selection (P=0.702) between *Oreothlypis celata* sequences and two sequences of the closely related *O. ruficapilla* (Lovette, Bermingham & Sheldon, 2002).

mtDNA haplotype network

Examination of the minimum-spanning haplotype network revealed incomplete sorting, regardless of how we grouped samples into populations (Figures 2, S3, and S4). The haplotypes clustered largely along a north-south geographic axis, but the majority of the Haida Gwaii *Oreothlypis celata* possessed haplotypes in the "southern" group. Three mutational differences

separate the major haplotype clusters of the northern and southern *O. celata* with some outlier individuals falling into each grouping.

The *Oreothlypis celata* haplotypes from the Channel Islands clustered much more tightly than those from Haida Gwaii. We found four *ND2* haplotypes among the Channel Islands *O. c. sordida*, but the majority of individuals shared a single haplotype; the three other Channel Islands haplotypes appeared only in one individual each (Figure 2). There was at most one mutational difference between the haplotype of a Channel Islands *O. celata* and the next Channel Islands haplotype. Although we found three singleton, private Channel Islands *ND2* haplotypes, individuals from northern and southern California shared the most common Channel Islands haplotype. The Haida Gwaii samples, with eleven haplotypes, were more loosely clustered than the Channel Islands samples with a maximum of nine mutational steps between individuals.

When we identified samples by subspecies, we found no interior *Oreothlypis celata orestera* individuals that shared haplotypes with the Channel Islands *O. c. sordida*. We did, however, find *O. c. orestera* haplotypes that were one mutational step away from *O. c. sordida* haplotypes (Figure S3). The main cluster of *O. c. lutescens* haplotype diversity was separated from the *O. c. sordida* haplotype cluster by a haplotype more often found in *O. c. orestera* than in *O. c. lutescens*. The haplotypes did not appear to cluster across a coast-interior axis (Figure S4). However, with the exception of one Haida Gwaii haplotype, the island populations of the Channel Islands and Haida Gwaii did not share haplotypes with any individuals from interior populations.

Population structure inferred from mtDNA

Variability in mtDNA sequences differed among populations (Table 1). We found that the Channel Islands population had the lowest nucleotide diversity (0.2×10^{-3}) of all eight

253 populations, whereas the northern California population had the highest (3.7×10^{-3}). The
254 nucleotide diversity of the Haida Gwaii population (2.8×10^{-3}) was substantially higher than that
255 of the Channel Islands populations and equaled that of the southern California population ($2.8 \times$
256 10^{-3}). When grouped into northern and southern population clusters, the two groupings contained
257 almost exactly the same nucleotide diversities (2.9×10^{-3} and 3.0×10^{-3}, respectively).

258 Although the minimum spanning networks (Figures 2, S3, and S4) did not display
259 evidence of reciprocal monophyly or complete lineage sorting, the F_{ST} and AMOVA estimates
260 revealed differentiation in haplotype frequencies. The overall F_{ST} estimates from our analysis of
261 *ND2* sequences for samples grouped into northern and southern clusters, eight populations,
262 coastal and interior clusters, and subspecies (0.191, 0.202, 0.186, 0.195, respectively) were all
263 highly significant ($p < 0.01$). Overall Φ_{ST} estimates were greater than the F_{ST} estimates for the
264 northern-southern, eight-population, coastal-interior, and subspecies population datasets (0.429,
265 0.365, 0.254, 0.299, respectively) and were also all highly significant with $p < 0.01$. The overall
266 Φ_{ST} estimates displayed a slightly different pattern than the overall F_{ST}. Overall Φ_{ST} was greatest
267 when comparing northern versus southern samples, whereas overall F_{ST} was highest when we
268 divided the samples into eight populations. However, the pairwise population F_{ST} values
269 reflected patterns that were nearly congruent to the pairwise Φ_{ST} estimates, so we have chosen to
270 present only the pairwise Φ_{ST} estimates (Tables 3 and 4).

271 Pairwise population F_{ST} and Φ_{ST} estimates (0.036 and 0.000, respectively) between Santa
272 Cruz Island (northern Channel Islands) and Santa Catalina Island (southern Channel Islands)
273 were not significant. However, pairwise Φ_{ST} estimates supported the collective Channel Islands
274 as a distinct population. Pairwise Φ_{ST} values between the Channel Islands and every other
275 population were significant, ranging from 0.245 to 0.809 with the samples grouped into eight

populations (Table 2) and from 0.228 to 0.681 with the samples grouped into northern and southern clusters (Table 3). With the samples grouped into eight populations, we estimated the highest pairwise Φ_{ST} values between the Channel Islands and the two northern, interior populations (Fairbanks, 0.809; Northern Rocky Mountains, 0.754). Of all of the pairwise comparisons involving the Channel Islands, we estimated the lowest Φ_{ST} between the Channel Islands and the northern and southern California populations (0.245 and 0.261, respectively). With the samples grouped by subspecies, we estimated significant pairwise Φ_{ST} between *Oreothlypis c. sordida* and all other subspecies, with the lowest values between *O. c. sordida* and *O. c. lutescens* (0.232) and the highest between *O. c. sordida* and *O. c. celata* (0.786; Table S2). *Oreothlypis c. lutescens* and *O. c. orestera* had the lowest pairwise Φ_{ST} value of all of the subspecies comparisons. All of the pairwise Φ_{ST} estimates were significant when we grouped the samples by subspecies (Table S2) and by coastal versus interior populations (Table S3).

Pairwise Φ_{ST} estimates between Haida Gwaii and every other population within the set of eight populations were significant, except for those between Haida Gwaii and the northern and southern California populations. Of all of the Haida Gwaii pairwise comparisons, pairwise Φ_{ST} was highest (0.564) between the Haida Gwaii and Channel Islands populations. The pairwise Φ_{ST} estimate was significant between the northern and southern populations (0.479; Table 3), but it was not as high as the estimate between the northern and Haida Gwaii populations (0.492). In contrast, pairwise Φ_{ST} was much lower between Haida Gwaii and the southern population (0.094; Table 3).

SAMOVA

As we found with our maximum parsimony and maximum likelihood analyses, our SAMOVA analyses indicated that deep genetic structure is not present in our mitochondrial

299 sequence data set. We never obtained a maximized F_{CT} with the SAMOVA analyses, so we
300 could not reject panmixia or obtain support for population structure greater than K=1. SAMOVA
301 is known to perform poorly in the presence of isolation by distance (Dupanloup, Schneider &
302 Excoffier, 2002) and we recovered significant isolation by distance in the microsatellite data.
303 However, the trend was weak and likely did not greatly affect the SAMOVA analyses. Although
304 we never recovered a maximized F_{CT} with the SAMOVA analyses, we examined the groupings
305 created for K=2-4 to see whether the analyses recovered any divisions between northern,
306 southern, and island samples. These analyses partitioned the samples in general agreement with
307 our northern and southern sample groupings. For K=2, we recovered one group composed
308 entirely of northern samples. The second group included all of the southern, Channel Islands, and
309 Haida Gwaii samples as well as samples from five coastal and interior localities (in British
310 Columbia, Alberta, and Fairbanks) in our designated northern population. Grouping samples
311 with K=3 and K=4 created partitions within the northern and southern populations.
312 *Mismatch distributions*
313 Mismatch profiles that follow a Poisson distribution suggest population growth following
314 an event such as a range expansion (Rogers & Harpending, 1992; Harpending et al., 1993).
315 Multimodal mismatch profiles can suggest a number of different population dynamic scenarios,
316 such as constant size (Slatkin & Hudson, 1991; Rogers & Harpending, 1992; Harpending et al.,
317 1998), expanding fronts (Liebers, Helbig & De Knijff, 2001), and geographic structuring
318 resulting from restricted gene flow (Marjoram & Donnelly, 1994). All populations had negative
319 Tajima and Fu statistics and all were statistically significant with the exception of the Fairbanks
320 and Northern Rocky Mountains populations for Tajima's D and the southern California
321 population for Fu's F (Table 1). Harpending's Raggedness indices were not statistically

significant for mismatch distributions in any of the populations, indicating that we could not reject a population expansion hypothesis (Table 1). The northern, southern, and Channel Islands populations displayed mismatch profiles following a Poisson distribution, suggesting recent population growth (Figure S5). With the samples grouped into eight populations, we observed mismatch profiles with a Poisson distribution in all populations except the Fairbanks and Haida Gwaii populations, both of which appeared to have multimodal mismatch profiles (Figure S5).

Population structure inferred from microsatellite data

We successfully obtained genotypes for 192 *Oreothlypis celata* individuals at ten microsatellite loci with no missing data apart from three individuals for which we were unable to genotype a subset of the loci (Tables 4, S4, and S5). We found no evidence for null alleles in any microsatellite locus in any population. In addition, there was no evidence for linkage disequilibrium in the northern, southern, Channel Islands, or Haida Gwaii populations; no disequilibrium tests were significant after we applied Bonferroni corrections. We did not observe deviation of observed heterozygosity from Hardy-Weinberg equilibrium (HWE) expectations repeatedly across loci in any of the populations resulting from our various methods of sample grouping. Observed heterozygosity at all ten loci did not differ from that expected under HWE for the northern, southern, Channel Island, and Haida Gwaii population set. However, locus Vce34 was out of HWE in the Fairbanks population, locus Vce167 was out of HWE in the interior population, and locus Vce34 was out of HWE in the *O. c. celata* population.

The overall F_{ST} estimates from our analysis of microsatellite genotypes for the northern-southern, eight-population, coastal-interior, and subspecies population sets (0.017, 0.022, 0.016, 0.020, respectively) were all highly significant ($p < 0.001$). Overall R_{ST} estimates were also highly significant ($p < 0.001$), exhibiting the same pattern as the F_{ST} estimates and exceeded

these for the northern-southern, eight-population, coastal-interior, and subspecies population sets (0.055, 0.068, 0.053, 0.058, respectively).

Both the pairwise F_{ST} and R_{ST} estimates from our microsatellite data displayed patterns almost congruent to the pairwise F_{ST} and Φ_{ST} estimates obtained from the mtDNA data. As with the pairwise F_{ST} and Φ_{ST} estimates for the mtDNA data, the pairwise population F_{ST} values were smaller than and showed patterns similar to the pairwise R_{ST} estimates, so we chose to present only pairwise R_{ST} estimates (Tables 2, 3, S2, and S3) here. As with the pairwise Φ_{ST} estimates, the pairwise R_{ST} estimates supported the existence of a distinct Channel Islands population. In further agreement with the mtDNA analyses, the pairwise F_{ST} and R_{ST} estimates between Santa Cruz Island and Santa Catalina Island (representing the northern and southern Channel Islands, respectively) were not statistically significant. Pairwise R_{ST} estimates between the Channel Islands population and the northern, southern, and Haida Gwaii populations were significant at 0.130, 0.091, and 0.178, respectively (Table 3). When we grouped samples into eight populations, pairwise R_{ST} values between the Channel Islands and every other population, except for southern California, were significant, ranging from 0.027 to 0.221 (Table 2). Within the set of eight populations, the highest pairwise R_{ST} estimate (0.221) was between the Channel Islands and Fairbanks populations. Of the pairwise comparisons amongst the set of eight populations that included the Channel Islands, the lowest pairwise R_{ST} estimate (0.027) was between the Channel Islands and southern California populations; the second-lowest estimate (0.094) was between the Channel Islands and Northern Rocky Mountains. Across all loci, we identified three private alleles in the Channel Islands and four in Haida Gwaii, whereas we found only two private alleles in the southern California population (Table S4). When we grouped samples by subspecies, the highest of the pairwise R_{ST} estimates involving *O. c. sordida* (0.187) was

368 between *O. c. sordida* and *O. c. celata*. The lowest of these estimates (0.105) was between *O. c.*
369 *sordida* and *O. c. orestera*, but the estimate between *O. c. sordida* and *O. c. lutescens* (0.106)
370 was very close (Table S2).

371 When we grouped samples into northern, southern, Channel Islands, and Haida Gwaii
372 populations, we found that the pairwise R_{ST} estimates between Haida Gwaii and the southern
373 population, but not between Haida Gwaii and the northern population nor between the northern
374 and southern populations, were significant. When we grouped the samples into eight populations,
375 the pairwise R_{ST} estimates involving the Haida Gwaii population ranged from 0.002 with the
376 Northern Rocky Mountains to 0.177 with the Channel Islands; estimates were significant with all
377 populations, except for Fairbanks, the Northern Rocky Mountains, and northern California
378 (Table 2). The pairwise R_{ST} estimates did not suggest much differentiation within the northern
379 populations, as none of the pairwise R_{ST} estimates involving the Fairbanks, Haida Gwaii,
380 Northern Rocky Mountains, and northern California populations were statistically significant
381 (Table 2). The insignificant pairwise R_{ST} estimate between the Southern Rocky Mountains and
382 Nevada suggested a connection between these populations; pairwise R_{ST} estimates between them
383 and all other populations, except for the Northern Rocky Mountains, were significant (Table 2).

384 Overall, the microsatellite data revealed little genetic structure and low divergence of
385 populations among our *Oreothlypis celata* samples. Our PCA analysis did not reveal distinct
386 clustering of the samples by population. Mantel tests utilizing geographic distance (GGD) and
387 Log(1+GGD) versus genetic distance (GD) resulted in weak, statistically significant, positive
388 correlation between geographical distance of *O. celata* sampling localities and genetic distance
389 measured at microsatellite loci (r^2=0.015, P=0.006 for GGD vs. GD and r^2=0.031, P=0.001 for
390 Log(1+GGD) vs. GD). Our preliminary Structure analyses, in which we did not provide any a

priori population information, suggested K=1 as the optimal number of genetic clusters. When we grouped the samples into eight pre-designated populations, the mean ln Pr(X | K) and ΔK (Evanno, Regnaut & Goudet, 2005) suggested K=2 as the optimal number of genetic clusters (Figure 3). All of the Channel Islands samples had high ancestry (> 83%) in one of the clusters, whereas the northernmost samples had the highest ancestry in the other cluster. In our analysis of substructure within the seven populations other than the Channel Islands, ΔK suggested K=2 as optimal, but the highest mean ln Pr(X | K) was for K=1, although the log probability for K=2 was very similar. With K=2, the southern California, Nevada, and Southern Rocky Mountains populations had high ancestry in one of the clusters and the northern California, Northern Rocky Mountains, Haida Gwaii, and Fairbanks populations had similarly high ancestry in the other genetic cluster (Figure S6). In our analysis of substructure within the Channel Islands samples, ΔK suggested K=4 as optimal, but the highest mean ln Pr(X | K) was for K=1.

Migration rate estimates

Our IMa2p analyses obtained an upper bound to the effective size of the Channel Islands population, but the analyses did not converge on an upper bound to the effective size of the mainland southern California population. This suggests that the effective size of the mainland population is likely much higher than that of the Channel Islands. Even though we were unable to effectively calculate migration rates scaled by population size, we were still able to assess the relative population sizes and rates of migration between the two populations. Across all three runs, we calculated a pairwise probability of 1.000 that the current effective population size of the southern California population is greater than that of the Channel Islands population. The probability that the current effective population size of the Channel Islands population is greater than that of the southern California population was < 0.001. Our migration rate estimates were

414 similar across our three IMa2p runs. Across all three runs, we estimated probabilities of 0.986 to
415 1.000 that the rate at which (looking forward in time) the southern California population receives
416 genes from the Channel Islands population is greater than that of the reverse direction. Inversely,
417 we calculated probabilities ranging from 0.000-0.013 that the rate at which (looking forward in
418 time) the Channel Islands receives genes from southern California is greater than migration in
419 the reverse direction.

420 **Discussion**

421 Genetic analyses of population structure in *Oreothlypis celata* revealed some structure in
422 portions of the range and high levels of shared alleles due to incomplete lineage sorting across
423 much of the mainland distribution of *O. celata*. In general, the mitochondrial data suggested
424 higher pairwise divergences among populations than the microsatellite data. The mitochondrial,
425 but not the microsatellite data, supported statistically significant divergence between northern
426 and southern *O. celata*. The microsatellite data provided support for statistically significant, but
427 weak, isolation by distance. Both the mitochondrial and microsatellite data suggested that the
428 Channel Islands represent the most genetically distinct population included in our study. We
429 found the highest genetic divergence between the Channel Islands and Fairbanks populations, the
430 two most geographically distant populations in our analyses.

431 Both the mtDNA and microsatellite data suggested that the Channel Islands *Oreothlypis*
432 *celata* comprise a separate population that is distinct from the mainland population. A notable
433 lack of *ND2* haplotype diversity (four haplotypes in 30 individuals with 27 individuals sharing
434 the same haplotype) in the Channel Islands is suggestive of a recent founder event, bottleneck, or
435 strong selection. The nucleotide diversity within all other populations was much higher than that
436 of the Channel Islands. Within the Channel Islands, the northern and southern island populations

(represented by samples from Santa Cruz Island and Santa Catalina Island, respectively) did not display divergence in pairwise F_{ST} or Φ_{ST} comparisons of the mtDNA gene *ND2* or in pairwise F_{ST} or R_{ST} comparisons of microsatellite data. Sequences from both islands clustered in our phylogenetic trees and haplotype network, suggesting that *O. c. sordida* from the northern and southern Channel Islands constitute one large population. The *O. c. sordida* individuals from Santa Cruz Island all shared the same *ND2* haplotype, which was also present on Santa Catalina Island. We identified three additional *ND2* haplotypes unique to Santa Catalina Island. The difference in haplotype diversity could be merely a sampling artifact, but this is unlikely given our sample size of 15 individuals from each island. Although the northern and southern Channel Islands may, in fact, be two separate populations that are diverging, any divergence is likely too recent to be statistically detected with our genetic data, despite the high mutation rates of our markers.

In contrast with other subspecies of *Oreothlypis celata*, *O. c. sordida* from the Channel Islands do not undertake a lengthy migration, although individuals may move short distances outside of the breeding season (Gilbert, Sogge & Van Riper III, 2010). The non-migratory tendency of *O. c. sordida* and its smaller population size on the islands than on the mainland have both likely contributed to genetic differentiation of the Channel Islands population. Based on the distinct phenotypes of island *O. c. sordida* individuals, Johnson (1972) hypothesized that the Channel Islands *O. celata* populations have been isolated from the mainland for a substantial period of time. The presence of incomplete lineage sorting, the low degree of divergence and diversity in the mitochondrial data, and the paucity of private microsatellite alleles do not support his hypothesis; rather, they suggest that the phenotypic differences in the *O. c. sordida* populations are of relatively recently derivation.

We obtained evidence for significantly greater gene flow from the Channel Islands to mainland southern California than in the reverse direction, a pattern that has also been detected in horned larks (*Eremophila alpestris*) (Mason et al., 2014). Both mitochondrial and microsatellite data supported *O. c. sordida* being more closely allied to coastal *O. c. lutescens* populations than to those of the interior *O. c. orestera*, contradicting Johnson's (1972) hypothesis of a closer relationship between *O. c. orestera* and *O. c. sordida*. However, the Structure analysis in which we excluded the Channel Islands population suggested similar ancestry in the *O. c. lutescens* population of mainland southern California and the *O. c. orestera* populations of the Southern Rocky Mountains and Nevada (Figure S6).

Of the four *Oreothlypis celata* subspecies represented in our study, our molecular data most strongly supported *O. c. sordida* from the Channel Islands as a distinct group. Our finding of greater gene flow from the Channel Islands to mainland southern California than from the mainland to the islands supports the recognition that *O. c. sordida* also occurs restrictedly along the coast of mainland southern California (Dunn & Garrett, 1997). Although we obtained statistically significant pairwise divergences between all pairs of subspecies, except between *O. c. lutescens* and *O. c. celata*, using our microsatellite data, our other methods did not recover genetic clusters that clearly distinguished subspecies other than *O. c. sordida*. Ongoing gene flow between *O. celata* subspecies may be acting to prevent greater divergence of populations. Using microsatellite data, Bull et al. (2010) calculated significant gene flow from populations of *O. c. lutescens* into *O. c. celata*. Providing further evidence of gene flow between the two subspecies, Gilbert and West (2015) identified *O. celata* individuals from Alaska that were morphologically intermediate between *O. c. celata* and *O. c. lutescens*. Overall, our results suggest that the differentiation seen in phenotypic and ecologic characters across *O. celata* is recent. Similar to

the findings of Bull et al. (2010) for northern populations of *O. c. celata* and *O. c. lutescens*, our results are consistent with isolation by distance having generated the genetic distances and clusters we observed across the western North American range of *O. celata*.

Acknowledgements

We thank Anand Varma for permission to reproduce the photos included as Figures S1 and S2. For access to specimens and genetic samples, we thank Andrew Johnson, Alison Boyer, and the Museum of Southwestern Biology; Kevin Burns and the San Diego State University Museum of Biodiversity; Vicki Friesen, Kimberley Lemmen, Scott Taylor, Theresa Burg, and Roger Bull of Queen's University and the Canadian Museum of Nature; Jocelyn Hudon and the Royal Alberta Museum; and the Museum of Vertebrate Zoology. For assistance in the field, we thank Jessica Castillo and Janette Havens. We appreciate support provided by Mark R. Stromberg in our collection activities at Hastings Natural History Reservation. We thank Monica J. Albe for help with specimen preparations and field equipment, Lydia Smith for laboratory support, Michelle Koo for assistance with graphics construction, and Anna Sellas for advice regarding laboratory work and data analyses.

References

Bermingham E, Rohwer S, Freeman S, Wood C. 1992. Vicariance Biogeography in the Pleistocene and Speciation in North American Wood Warblers: A Test of Mengel's Model. *Proceedings of the National Academy of Sciences* 89:6624–6628.

Bowie RCK, Feldheim KA, Hanna ZR, Sellas AB, Cicero C. 2017. Development of Polymorphic Tetranucleotide Microsatellite Markers for New World Warblers (Aves: Passeriformes: Parulidae) with Broad Cross-species Utility. *The Wilson Journal of Ornithology* 129:401–407. DOI: 10.1676/16-110.1.

Brunsfeld SJ, Sullivan J, Soltis DE, Soltis PS. 2001. Comparative phylogeography of northwestern North America: a synthesis. In: *Integrating Ecology and Evolution in a Spatial Context*. Oxford: Blackwell Science, 319–340.

Bull RD, McCracken A, Gaston AJ, Birt TP, Friesen VL. 2010. Evidence of Recent Population Differentiation in Orange-crowned Warblers (*Vermivora celata*) in Haida Gwaii. *The Auk* 127:23–34. DOI: 10.1525/auk.2009.09159.

Burg TM, Gaston AJ, Winker K, Friesen VL. 2006. Effects of Pleistocene glaciations on population structure of North American chestnut-backed chickadees. *Molecular Ecology* 15:2409–2419. DOI: 10.1111/j.1365-294X.2006.02957.x.

Caballero IC, Ashley MV. 2011. Genetic analysis of the endemic island loggerhead shrike, *Lanius ludovicianus anthonyi*. *Conservation Genetics* 12:1485–1493. DOI: 10.1007/s10592-011-0247-4.

Chhatre VE. 2016. Distruct. Version 2.2. [Accessed 2018 Jun 21]. Available from: http://www.crypticlineage.net/pages/distruct.html.

520 Chhatre VE, Emerson KJ. 2017. StrAuto: automation and parallelization of STRUCTURE
521 analysis. *BMC Bioinformatics* 18:192. DOI: 10.1186/s12859-017-1593-0.
522 Chhatre VE, Emerson KJ. 2018. StrAuto. Version 1.0. [Accessed 2018 Jun 21]. Available from:
523 http://www.crypticlineage.net/pages/software.html.
524 Clement M, Posada D, Crandall KA. 2000. TCS: a computer program to estimate gene
525 genealogies. *Molecular ecology* 9:1657–1659.
526 Crawford DJ. 2012. Oceanic islands as evolutionary laboratories. *Access Science*. DOI:
527 10.1036/1097-8542.YB120241.
528 Delaney KS, Zafar S, Wayne RK. 2008. Genetic Divergence and Differentiation within the
529 Western Scrub-Jay (*Aphelocoma californica*). *The Auk* 125:839–849. DOI:
530 10.1525/auk.2008.07088.
531 Diamond JM. 1969. Avifaunal Equilibria and Species Turnover Rates on the Channel Islands of
532 California. *Proceedings of the National Academy of Sciences* 64:57–63.
533 Dunn JL, Garrett KL. 1997. *A Field Guide to Warblers of North America*. New York, New York:
534 Houghton Mifflin Company.
535 Dupanloup I, Schneider S, Excoffier L. 2002. A simulated annealing approach to define the
536 genetic structure of populations. *Molecular Ecology* 11:2571–2581. DOI:
537 10.1046/j.1365-294X.2002.01650.x.
538 Earl D. 2014. Structure Harvester. Version 0.6.94. [Accessed 2018 Jun 21]. Available from:
539 https://github.com/dentearl/structureHarvester.
540 Earl DA, vonHoldt BM. 2012. STRUCTURE HARVESTER: a website and program for
541 visualizing STRUCTURE output and implementing the Evanno method. *Conservation*
542 *Genetics Resources* 4:359–361. DOI: 10.1007/s12686-011-9548-7.

543 Evanno G, Regnaut S, Goudet J. 2005. Detecting the number of clusters of individuals using the
544 software structure: a simulation study. *Molecular Ecology* 14:2611–2620. DOI:
545 10.1111/j.1365-294X.2005.02553.x.
546 Excoffier L, Laval G, Schneider S. 2007. Arlequin (version 3.0): An integrated software package
547 for population genetics data analysis. *Evolutionary Bioinformatics Online* 1:47–50.
548 Excoffier L, Smouse PE, Quattro JM. 1992. Analysis of molecular variance inferred from metric
549 distances among DNA haplotypes: application to human mitochondrial DNA restriction
550 data. *Genetics* 131:479–491.
551 Falush D, Stephens M, Pritchard JK. 2003. Inference of Population Structure Using Multilocus
552 Genotype Data: Linked Loci and Correlated Allele Frequencies. *Genetics* 164:1567–
553 1587.
554 Foster MS. 1967. Molt Cycles of the Orange-crowned Warbler. *The Condor* 69:169–200. DOI:
555 10.2307/1366606.
556 Fu Y-X. 1997. Statistical Tests of Neutrality of Mutations Against Population Growth,
557 Hitchhiking and Background Selection. *Genetics* 147:915–925.
558 Gilbert WM, Sogge MK, Van Riper III C. 2010. Orange-crowned Warbler (*Oreothlypis celata*),
559 version 2.0. In: *The Birds of North America (P. G. Rodewald, editor)*. Ithaca, New York,
560 U.S.A.: Cornell Lab of Ornithology,.
561 Gilbert WM, West GC. 2015. Morphological expression in putative intergrades between two
562 subspecies of Orange-crowned Warbler (*Oreothlypis celata*) on the Kenai Peninsula,
563 Alaska. *The Wilson Journal of Ornithology* 127:29–42. DOI: 10.1676/13-153.1.

564 Ginot F, Bordelais I, Nguyen S, Gyapay G. 1996. Correction of Some Genotyping Errors in
565 Automated Fluorescent Microsatellite Analysis by Enzymatic Removal of One Base
566 Overhangs. *Nucleic Acids Research* 24:540–541. DOI: 10.1093/nar/24.3.540.
567 Goodman SJ. 1997. RST Calc: a collection of computer programs for calculating estimates of
568 genetic differentiation from microsatellite data and determining their significance.
569 *Molecular Ecology* 6:881–885. DOI: 10.1111/j.1365-294X.1997.tb00143.x.
570 Goudet J. 1995. FSTAT (Version 1.2): A Computer Program to Calculate F-Statistics. *Journal of*
571 *Heredity* 86:485–486. DOI: 10.1093/oxfordjournals.jhered.a111627.
572 Goudet J. 2001. FSTAT. Version 2.9.3.2. A program to estimate and test gene diversities and
573 fixation indices. [Accessed 2017 Nov 21]. Available from:
574 http://www2.unil.ch/popgen/softwares/fstat.htm. *Lausanne University, Lausanne,*
575 *Switzerland*.
576 Greenberg R, Danner RM. 2013. Climate, ecological release and bill dimorphism in an island
577 songbird. *Biology Letters* 9. DOI: 10.1098/rsbl.2013.0118.
578 Gunderson AR, Mahler DL, Leal M. 2018. Thermal niche evolution across replicated *Anolis*
579 lizard adaptive radiations. *Proc. R. Soc. B* 285:20172241. DOI: 10.1098/rspb.2017.2241.
580 Hanna ZR, Cicero C, Bowie RCK. 2018. ocwa-popgen. *Zenodo*. DOI: 10.5281/zenodo.1648690.
581 Harpending HC, Batzer MA, Gurven M, Jorde LB, Rogers AR, Sherry ST. 1998. Genetic traces
582 of ancient demography. *Proceedings of the National Academy of Sciences* 95:1961–1967.
583 Harpending HC, Sherry ST, Rogers AR, Stoneking M. 1993. The Genetic Structure of Ancient
584 Human Populations. *Current Anthropology* 34:483–496. DOI: 10.2307/2743761.

585 Hubisz MJ, Falush D, Stephens M, Pritchard JK. 2009. Inferring weak population structure with
586 the assistance of sample group information. *Molecular Ecology Resources* 9:1322–1332.
587 DOI: 10.1111/j.1755-0998.2009.02591.x.
588 Jakobsson M, Rosenberg NA. 2007. CLUMPP: a cluster matching and permutation program for
589 dealing with label switching and multimodality in analysis of population structure.
590 *Bioinformatics* 23:1801–1806. DOI: 10.1093/bioinformatics/btm233.
591 Johnson NK. 1972. Origin and Differentiation of the Avifauna of the Channel Islands,
592 California. *The Condor* 74:295–315. DOI: 10.2307/1366591.
593 Jones HL, Diamond JM. 1976. Short-Time-Base Studies of Turnover in Breeding Bird
594 Populations on the California Channel Islands. *The Condor* 78:526–549. DOI:
595 10.2307/1367103.
596 Karin BR, Cicero C, Koo MS, Bowie RCK. 2018. The role of history and ecology as drivers of
597 song divergence in Bell's and Sagebrush sparrows (*Artemisiospiza*, Aves: Passerellidae).
598 *Biological Journal of the Linnean Society* 125:421–440. DOI:
599 10.1093/biolinnean/bly090.
600 Leberg PL. 2002. Estimating allelic richness: Effects of sample size and bottlenecks. *Molecular*
601 *Ecology* 11:2445–2449. DOI: 10.1046/j.1365-294X.2002.01612.x.
602 Liebers D, Helbig AJ, De Knijff P. 2001. Genetic differentiation and phylogeography of gulls in
603 the *Larus cachinnans–fuscus* group (Aves: Charadriiformes). *Molecular Ecology*
604 10:2447–2462. DOI: 10.1046/j.0962-1083.2001.01370.x.
605 Lomolino MV. 2005. Body size evolution in insular vertebrates: generality of the island rule.
606 *Journal of Biogeography* 32:1683–1699. DOI: 10.1111/j.1365-2699.2005.01314.x.

607 Losos JB, Ricklefs RE. 2009. Adaptation and diversification on islands. *Nature* 457:830–836.
608 DOI: 10.1038/nature07893.
609 Lovette IJ, Bermingham E, Sheldon F. 2002. What is a wood-warbler? molecular
610 characterization of a monophyletic parulidae. *The Auk* 119:695–714. DOI: 10.1642/0004-
611 8038(2002)119[0695:WIAWWM]2.0.CO;2.
612 Lynch JF, Johnson NK. 1974. Turnover and Equilibria in Insular Avifaunas, with Special
613 Reference to the California Channel Islands. *The Condor* 76:370–384. DOI:
614 10.2307/1365812.
615 Marjoram P, Donnelly P. 1994. Pairwise comparisons of mitochondrial DNA sequences in
616 subdivided populations and implications for early human evolution. *Genetics* 136:673–
617 683.
618 Mason NA, Title PO, Cicero C, Burns KJ, Bowie RCK. 2014. Genetic variation among western
619 populations of the Horned Lark (*Eremophila alpestris*) indicates recent colonization of
620 the Channel Islands off southern California, mainland-bound dispersal, and postglacial
621 range shifts. *The Auk* 131:162–174. DOI: 10.1642/AUK-13-181.1.
622 Mundy NI, Winchell CS, Woodruff DS. 1997. Genetic differences between the endangered San
623 Clemente Island loggerhead shrike *Lanius ludovicianus mearnsi* and two neighbouring
624 subspecies demonstrated by mtDNA control region and *cytochrome b* sequence variation.
625 *Molecular Ecology* 6:29–37. DOI: 10.1046/j.1365-294X.1997.00149.x.
626 Nei M. 1972. Genetic Distance between Populations. *The American Naturalist* 106:283–292.
627 DOI: 10.2307/2459777.
628 Nei M. 1987. *Molecular Evolutionary Genetics*. New York, New York: Columbia University
629 Press.

630 Oberholser HC. 1905. The Forms of *Vermivora celata* (Say). *The Auk* 22:242–247. DOI:
631 10.2307/4070156.
632 Peakall R, Smouse PE. 2006. genalex 6: genetic analysis in Excel. Population genetic software
633 for teaching and research. *Molecular Ecology Notes* 6:288–295. DOI: 10.1111/j.1471-
634 8286.2005.01155.x.
635 Peakall R, Smouse PE. 2012. GenAlEx 6.5: genetic analysis in Excel. Population genetic
636 software for teaching and research—an update. *Bioinformatics* 28:2537–2539. DOI:
637 10.1093/bioinformatics/bts460.
638 Posada D, Crandall KA. 2001. Intraspecific gene genealogies: trees grafting into networks.
639 *Trends in Ecology & Evolution* 16:37–45. DOI: 10.1016/S0169-5347(00)02026-7.
640 Pritchard JK, Falush D, Hubisz MJ. 2012. Structure. Version 2.3.4. [Accessed 2018 Jun 21].
641 Available from: https://web.stanford.edu/group/pritchardlab/structure.html.
642 Pritchard JK, Stephens M, Donnelly P. 2000. Inference of Population Structure Using Multilocus
643 Genotype Data. *Genetics* 155:945–959.
644 Raj A, Stephens M, Pritchard JK. 2014. fastSTRUCTURE: Variational Inference of Population
645 Structure in Large SNP Data Sets. *Genetics* 197:573–589. DOI:
646 10.1534/genetics.114.164350.
647 Raymond M, Rousset F. 1995. GENEPOP (Version 1.2): Population Genetics Software for Exact
648 Tests and Ecumenicism. *Journal of Heredity* 86:248–249.
649 Rice WR. 1989. Analyzing Tables of Statistical Tests. *Evolution* 43:223. DOI: 10.2307/2409177.
650 Ridgway R. 1872. *Helminthophaga celata* var. *lutescens*. In: *The American Journal of Science*
651 *and Arts*. Third Series. Volume 4. New Haven: Tuttle, Morehouse & Taylor, 457.

652 Rogers AR, Harpending H. 1992. Population growth makes waves in the distribution of pairwise
653 genetic differences. *Molecular Biology and Evolution* 9:552–569.
654 Rousset F. 2008. GENEPOP'007: a complete re-implementation of the GENEPOP software for
655 Windows and Linux. *Molecular Ecology Resources* 8:103–106. DOI: 10.1111/j.1471-
656 8286.2007.01931.x.
657 Say T. 1823. *Sylvia celatus*. In: *Account of an expedition from Pittsburgh to the Rocky*
658 *Mountains, performed in the years 1819 and '20, by order of the Hon. J.C. Calhoun,*
659 *Sec'y of War: under the command of Major Stephen H. Long. From the notes of Major*
660 *Long, Mr. T. Say, and other gentlemen of the exploring party. Compiled by Edwin James,*
661 *Botanist and Geologist for the expedition*. Volume 1. Philadelphia: H.C. Carey and I.
662 Lea, 169.
663 Schoenherr AA, Feldmeth CR, Emerson MJ. 1999. *Natural history of the islands of California*.
664 Berkeley and Los Angeles, California: University of California Press.
665 Sethuraman A. 2017. IMa2p. Version 58a02604e58b6a2bc3c1ccbb75767dafbb6fa781.
666 [Accessed 2018 Jun 21]. Available from: https://github.com/arunsethuraman/ima2p.
667 Sethuraman A, Hey J. 2015. IMa2p – parallel MCMC and inference of ancient demography
668 under the Isolation with migration (IM) model. *Molecular Ecology Resources* 16:206–
669 215. DOI: 10.1111/1755-0998.12437.
670 Slatkin M, Hudson RR. 1991. Pairwise comparisons of mitochondrial DNA sequences in stable
671 and exponentially growing populations. *Genetics* 129:555–562.
672 Soltis DE, Gitzendanner MA, Strenge DD, Soltis PS. 1997. Chloroplast DNA intraspecific
673 phylogeography of plants from the Pacific Northwest of North America. *Plant*
674 *Systematics and Evolution* 206:353–373. DOI: 10.1007/BF00987957.

675 Sorenson MD, Ast JC, Dimcheff DE, Yuri T, Mindell DP. 1999. Primers for a PCR-Based
676 Approach to Mitochondrial Genome Sequencing in Birds and Other Vertebrates.
677 *Molecular Phylogenetics and Evolution* 12:105–114. DOI: 10.1006/mpev.1998.0602.
678 Stamatakis A, Hoover P, Rougemont J. 2008. A Rapid Bootstrap Algorithm for the RAxML
679 Web Servers. *Systematic Biology* 57:758–771. DOI: 10.1080/10635150802429642.
680 Swenson NG, Howard DJ. 2005. Clustering of Contact Zones, Hybrid Zones, and
681 Phylogeographic Breaks in North America. *The American Naturalist* 166:581–591. DOI:
682 10.1086/491688.
683 Swofford DL. 2003. *PAUP*. Phylogenetic Analysis Using Parsimony (*and Other Methods)*.
684 *Version 4*. Sinauer Associates, Sunderland, Massachusetts.
685 Tajima F. 1989. Statistical method for testing the neutral mutation hypothesis by DNA
686 polymorphism. *Genetics* 123:585–595.
687 Tange O. 2011. GNU Parallel: The Command-Line Power Tool. ;*login: The USENIX Magazine*
688 36:42–47.
689 Townsend CH. 1890. *Helminthophila celata sordida*. In: *Proceedings of the United States*
690 *National Museum*. Volume 13. Washington, D.C.: Government Printing Office, 139.
691 Van Oosterhout C, Hutchinson WF, Wills DPM, Shipley P. 2004. MICRO-CHECKER: software
692 for identifying and correcting genotyping errors in microsatellite data. *Molecular Ecology*
693 *Notes* 4:535–538. DOI: 10.1111/j.1471-8286.2004.00684.x.
694 Wilson A, Arcese P, Keller LF, Pruett CL, Winker K, Patten MA, Chan Y. 2009. The
695 contribution of island populations to in situ genetic conservation. *Conservation Genetics*
696 10:419. DOI: 10.1007/s10592-008-9612-3.
697

Figure 1

Sample map and microsatellite allele pie charts.

Depicted here are all *Oreothlypis celata* sampling localities and the associated population designations used in this study. Population numbers correspond to the "Pop #" column in Table 1. We also provide an across-population comparison of the percent prevalence of a subset of the alleles found in our samples for the three most variable (Vce102, Vce128, and Vce167) and three least variable (Vce34, Vce70, and Vce179) loci. For each population, we present the percent prevalence of both the three most common and the rare alleles. We define rare alleles as those whose average occurrence in populations represents less than 5% of the allele pool. Loci Vce70 and Vce102 were exceptions to this definition. Due to the small total number, we included all five detected alleles for Vce70. There were so many rare alleles for Vce102 that we defined the rare alleles for this locus as those with an average population occurrence of < 1% of the total allele pool. For the least variable loci, we depict the percent prevalence of the three most common alleles and the rare alleles together in the same pie chart. Due to the large number of rare alleles in the most variable loci, we have depicted the rare alleles in a separate pie chart. For Vce102, Vce128, and Vce167, the left pie charts display the percent prevalence of the three most common alleles and the right graphs represent the percent prevalence of the rare alleles. The prevalence percentages depicted in the pie charts are all relative as the total prevalence of all alleles must sum to one. We recommend that the reader compare graphs vertically, across populations. A given color represents different alleles across columns.

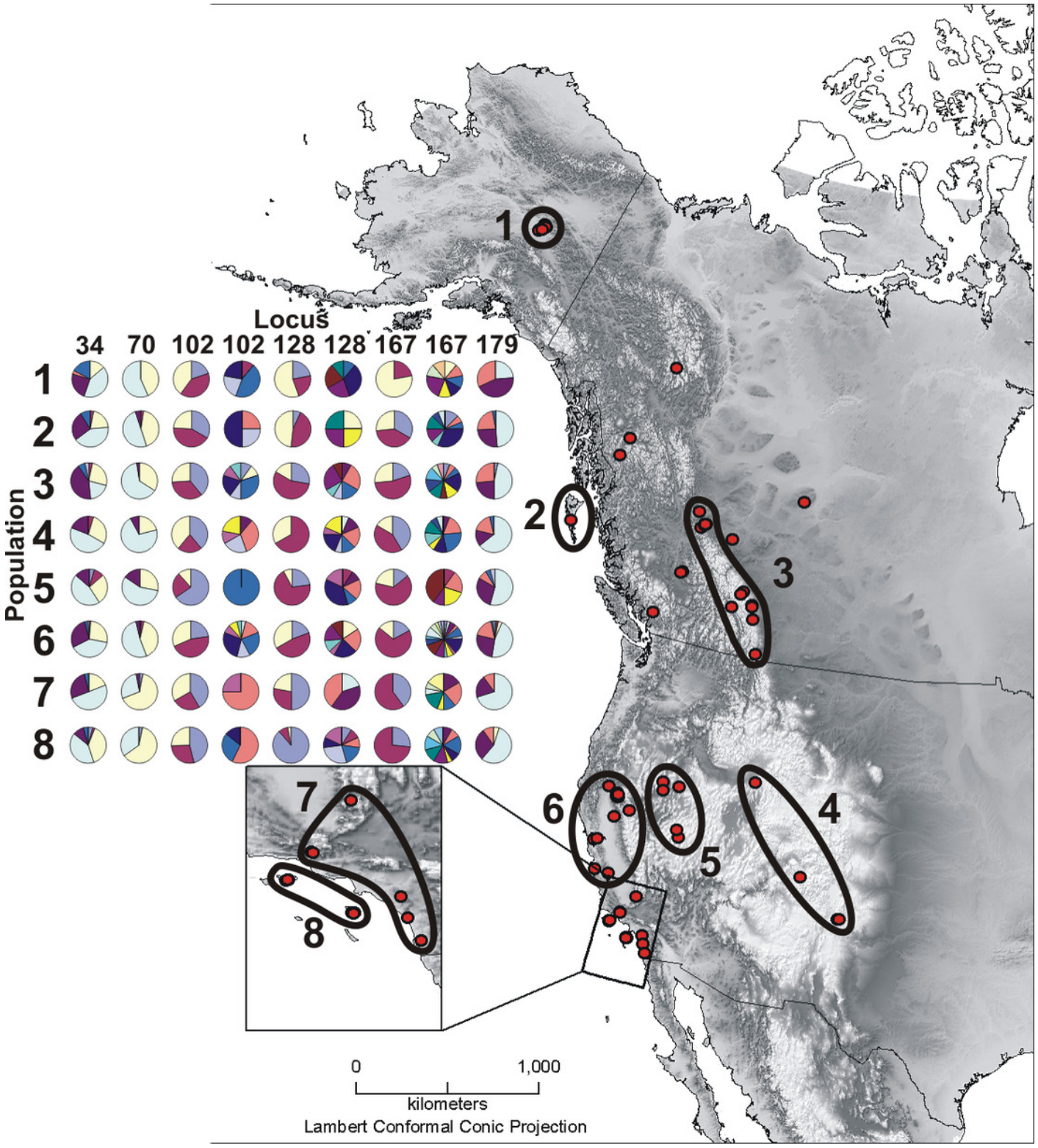

Figure 2

ND2 haplotype network.

We have shaded the left *ND2* haplotype network according to samples' designation in the northern or southern population. The coloring of the right haplotype network uses sample assignment under the eight population grouping arrangement, a more fine-scale partitioning than the north-south grouping schema. The haplotype numbers in the right graphic correspond with the numbers in Table S1. Circle sizes are proportional to the number of individuals with each haplotype. Lines connect haplotypes that differ by one mutation. Dots represent inferred haplotypes. Hash marks indicate the number of mutations between haplotypes separated by more than one mutational difference. For one circle of each size, we have labeled the number of individuals represented by that circle following "n=".

PeerJ Preprints | https://doi.org/10.7287/peerj.preprints.27418v1 | CC BY 4.0 Open Access | rec: 7 Dec 2018, publ: 7 Dec 2018

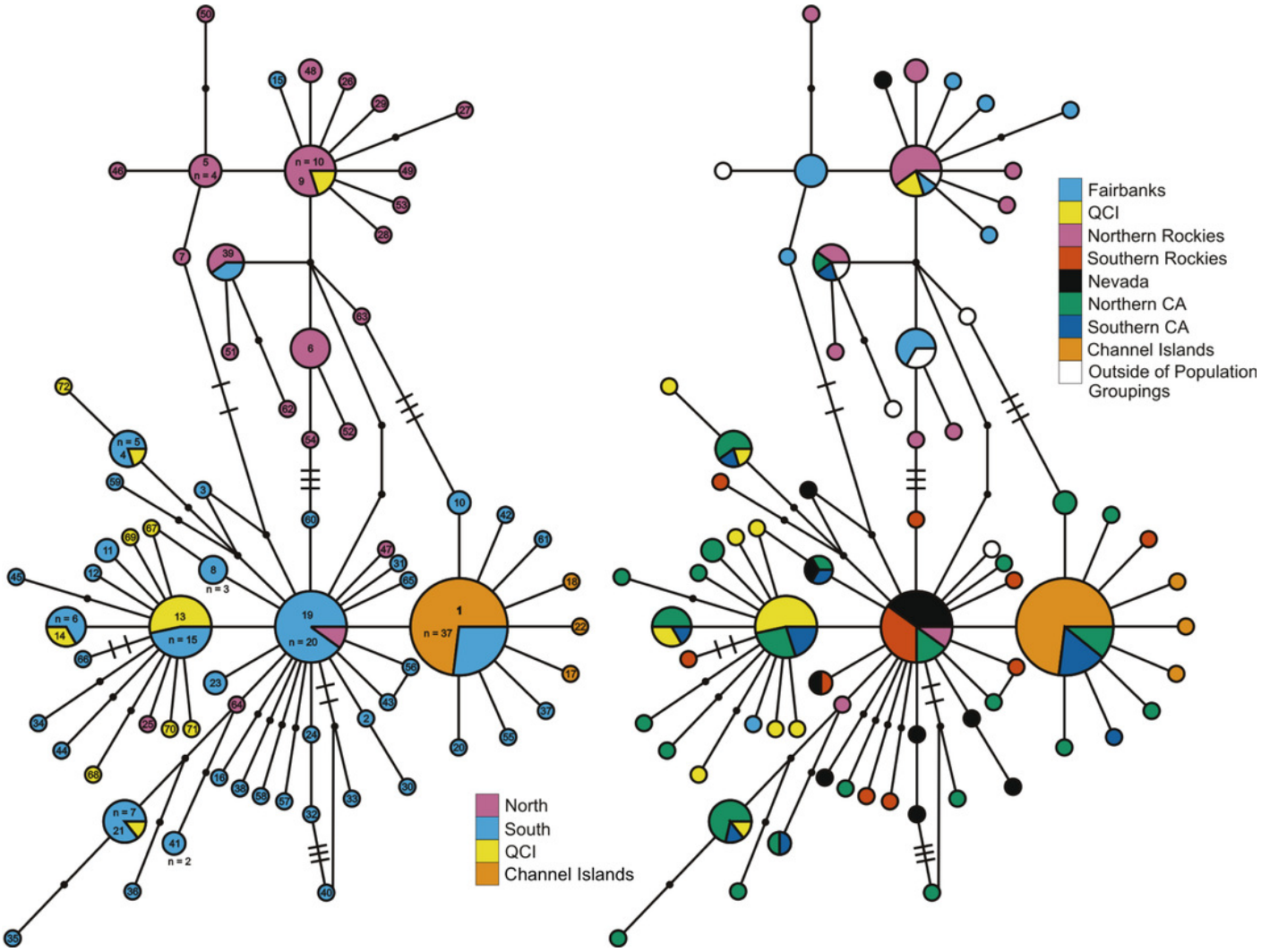
n = 10
n = 4
n = 5
n = 3
n = 6
n = 15
n = 20
n = 37
n = 7
n = 2
North
South
QCI
Channel Islands
Fairbanks
QCI
Northern Rockies
Southern Rockies
Nevada
Northern CA
Southern CA
Channel Islands
Outside of Population Groupings

Figure 3

Structure plot for *K*=2 with Channel Islands population included.

Different colors represent the two genetic clusters identified by Structure. Each vertical bar represents an individual *Oreothlypis celata*. The height of each color in a given bar illustrates the proportion of ancestry derived from each genetic cluster for that individual.

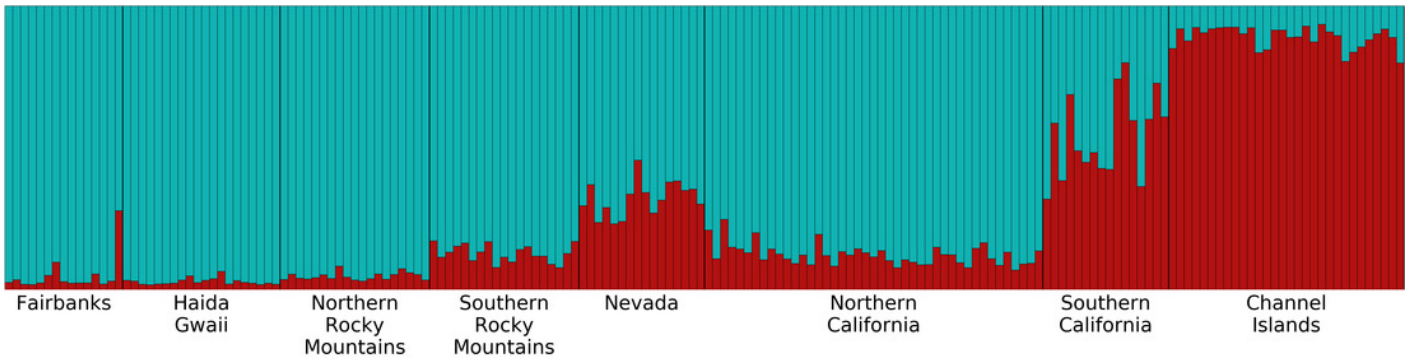

Table 1(on next page)

Microchondrial sequence data summary statistics.

This table presents summary statistics for the *ND2* mitochondrial sequence data for each population. We list the number of individuals sampled (*N*) and the number of haplotypes in each population. We provide estimates of haplotype diversity (*h*) with standard deviation, nucleotide diversity (π) with standard deviation, Tajima's D, Fu's Fs, and Harpending's Raggedness Index. The named "North" population includes Pop 1 and 3. The "South" population includes Pop 4 through 7. Values followed by one asterisk are significant with $p < 0.05$ and values followed by two asterisks are significant with $p < 0.001$.

Pop #	Population	*N*	Number of haplotypes	*h*	π	Tajima's D	Fu's Fs	Harpending's Raggedness Index
	North	42	23	0.94+/-0.02	0.0029+/-0.0017	-1.80*	-16.50**	0.023
	South	92	42	0.94+/-0.01	0.0030+/-0.0017	-2.35**	-26.42**	0.018
1	Fairbanks	15	9	0.89+/-0.06	0.0027+/-0.0017	-1.16	-3.05*	0.126
2	Haida Gwaii	20	11	0.84+/-0.08	0.0028+/-0.0017	-1.73*	-4.04*	0.063
3	Northern Rocky Mtns.	19	11	0.89+/-0.06	0.0029+/-0.0018	-1.31	-4.19*	0.030
4	Southern Rocky Mtns.	17	10	0.79+/-0.10	0.0019+/-0.0013	-2.25**	-5.44**	0.012
5	Nevada	16	10	0.83+/-0.10	0.0020+/-0.0013	-2.10*	-5.51**	0.041
6	Northern California	43	25	0.96+/-0.01	0.0037+/-0.0021	-2.07*	-16.47**	0.018
7	Southern California	16	9	0.85+/-0.08	0.0028+/-0.0017	-1.71*	-2.66	0.105
8	Channel Islands	30	4	0.19+/-0.10	0.0002+/-0.0003	-1.73*	-3.38**	0.417

1

Table 2 (on next page)

Population pairwise divergence statistics.

This table presents divergence statistics for pairwise population comparisons calculated using the *ND2* mitochondrial DNA sequence (Φ_{ST} above diagonal) and microsatellite data (R_{ST} below diagonal). Values followed by asterisks are significant after applying a Bonferroni correction ($p < 0.002$). See Table S1 for the samples included in each population.

	Fairbanks	Haida Gwaii	Northern Rocky Mountains	Southern Rocky Mountains	Nevada	Northern California	Southern California	Channel Islands
Fairbanks	-	0.525*	0.011	0.584*	0.532*	0.486*	0.528*	0.809*
Haida Gwaii	0.029	-	0.481*	0.152*	0.166*	0.061	0.110	0.564*
Northern Rocky Mountains	0.005	0.002	-	0.521*	0.467*	0.440*	0.472*	0.754*
Southern Rocky Mountains	0.119*	0.087*	0.026	-	0.006	0.016	0.047	0.531*
Nevada	0.141*	0.092*	0.033	0.000	-	0.035	0.069	0.558*
Northern California	0.027	0.020	0.000	0.038*	0.054*	-	0.000	0.245*
Southern California	0.103*	0.079*	0.025	0.089*	0.095*	0.040	-	0.261*
Channel Islands	0.221*	0.177*	0.094*	0.145*	0.123*	0.111*	0.027	-

1

Table 3(on next page)

Pairwise divergence statistics of the north, south, and island populations.

We here present the results of pairwise population comparisons with *ND2* mitochondrial DNA sequence (Φ_{ST} above diagonal) and microsatellite (R_{ST} below diagonal) data. Values followed by asterisks are significant after applying a Bonferroni correction ($p < 0.008$).

	North	South	Haida Gwaii	Channel Islands
North	-	0.479*	0.492*	0.681*
South	0.011	-	0.094*	0.228*
Haida Gwaii	0.013	0.038*	-	0.564*
Channel Islands	0.130*	0.091*	0.178*	-

1

Table 4(on next page)

Variability of the microsatellite loci in the north, south, and island populations.

This table presents the variability of the ten microsatellite loci in each of the four *Oreothlypis celata* populations in the North-South population schema. We indicate the number of individuals genotyped for each locus, "*N*". Column "A" provides the number of alleles at each locus in each population, with the number of private alleles given in parentheses. We also provide estimated values of allelic richness "R_S", observed heterozygosity "H_O", expected heterozygosity "H_E", and the associated *p*-values for each locus in each population. No *p*-values were significant after Bonferroni correction ($p < 0.005$).

Population	Locus	*N*	A (Private Alleles)	R_S	H_O	H_E	*p-val*
North							
	Vce34	43	10 (1)	8.51	0.698	0.827	0.085
	Vce50	43	37 (4)	24.14	0.953	0.966	0.738
	Vce70	42	4 (0)	3.66	0.452	0.555	0.177
	Vce102	42	12 (3)	9.664	0.738	0.836	0.223
	Vce103	42	8 (0)	7.011	0.571	0.640	0.059
	Vce109	42	10 (1)	8.331	0.833	0.833	0.381
	Vce116	42	10 (2)	8.146	0.786	0.839	0.331
	Vce128	42	18 (0)	14.43	0.857	0.924	0.211
	Vce167	43	23 (4)	17.00	0.814	0.915	0.097
	Vce179	43	8 (0)	6.869	0.860	0.788	0.190
South							
	Vce34	94	10 (0)	7.428	0.798	0.804	0.633
	Vce50	93	42 (7)	21.90	0.946	0.962	0.029
	Vce70	94	5 (0)	3.711	0.500	0.571	0.643
	Vce102	94	13 (3)	9.119	0.766	0.827	0.250
	Vce103	94	12 (3)	6.884	0.574	0.634	0.067
	Vce109	94	14 (3)	8.691	0.840	0.810	0.070
	Vce116	94	10 (1)	7.471	0.830	0.813	0.829
	Vce128	94	20 (0)	13.31	0.883	0.892	0.141
	Vce167	94	28 (6)	17.08	0.872	0.914	0.569
	Vce179	94	11 (2)	7.593	0.840	0.779	0.424
Haida Gwaii							
	Vce34	20	7 (0)	7.000	0.650	0.797	0.277
	Vce50	20	24 (3)	24.00	1.000	0.962	1.000
	Vce70	20	4 (0)	4.000	0.550	0.581	0.141
	Vce102	20	7 (0)	7.000	0.550	0.772	0.064
	Vce103	20	8 (0)	8.000	0.650	0.669	0.899
	Vce109	20	9 (0)	9.000	0.700	0.853	0.029
	Vce116	20	7 (1)	7.000	0.900	0.792	0.224
	Vce128	20	9 (0)	9.000	0.750	0.768	0.493
	Vce167	20	16 (0)	16.00	0.900	0.935	0.813
	Vce179	20	7 (0)	7.000	0.650	0.740	0.271
Channel Islands							
	Vce34	30	9 (0)	8.308	0.700	0.779	0.364
	Vce50	30	23 (2)	19.18	0.900	0.945	0.562
	Vce70	30	3 (0)	2.893	0.500	0.505	0.725
	Vce102	30	7 (0)	6.549	0.800	0.802	0.375
	Vce103	30	2 (0)	2.000	0.467	0.364	0.295
	Vce109	30	8 (0)	7.678	0.833	0.829	0.650
	Vce116	30	8 (0)	7.409	0.700	0.789	0.144
	Vce128	29	14 (1)	11.85	0.724	0.704	0.467
	Vce167	29	15 (0)	13.82	0.655	0.902	0.006
	Vce179	30	7 (0)	6.549	0.833	0.775	0.820

1